Electronic Supplementary Material (ESI) for Physical Chemistry Chemical Physics

Photoisomerisation Quantum Yield and Non-linear Cross-Sections with Femtosecond Excitation of the Photoactive Yellow Protein

Craig N. Lincoln,[a] Ann E. Fitzpatrick[a] and Jasper J. van Thor*[a]

Supporting Information

S1.1 Data Processing

Transient absorption signals resulting from long lived species, i.e., observed before time zero, were found to be less than one percent of the maximum signal at time zero. These signals were removed by subtracting the signal before time zero over all measured time delays. The transient absorption traces were 'chirp' corrected using the inbuilt function of a freeware global analysis toolbox developed in the Matlab environment.[1] The function fits an nth order polynomial to the peak signal around time zero to extract the time delay as a function of wavelength. The final 'chirp' corrected data was straightened using these wavelength dependent time delays through interpolation. Any incomplete spectra after straightening were removed. Signal corrupted by scattered pump impinging on the camera, was given a zero value. For the three experimental pump wavelengths (400, 450 and 490) the pump scatter ranges were 395-410 nm, 440-460 nm and 480-507 nm, respectively. Finally, all data were normalised using their corresponding linear absorption measured at 446 nm.

The transient absorption data were prepared as both time- and power-dependent datasets. In the case were *m* probe delay times and *n* excitation powers were measured the time-dependent data were organised into *n* matrices of *m* time-dependent spectra while the power-dependent data were *m* matrices of *n* power-dependent spectra.

S1.2 Data Analysis

All evolution dependent analysis was performed using a freeware global analysis toolbox developed within a Matlab environment. A detailed explanation can be found in Ref [1]. This program provides an easy to navigate GUI for the global fitting of transient absorption data employing the inbuilt *mldivide* function of Matlab to solve using the least squares procedure the system of equations described by $AX = B$, where A is a matrix containing transient absorption spectra, B is a column vector containing m time-dependent concentration profiles and the solution X is m time-independent spectra for each m time-dependent concentration profile. Evolution associated spectra were fitted using a sequential model that follows states $A(\tau_A) \rightarrow B(\tau_B) \rightarrow C(\tau_C) \rightarrow \ldots$ with associated decay times τ_{state}.

The transient absorption data were separated into components corresponding to one- and stepwise multi-photon dependent spectra using the following method. Power-dependent concentration curves were extracted by taking the maximum amplitude at wavelengths 386 nm and 670 nm over all probe delay times for each excitation power. The first wavelength of 386 nm corresponds to near peak amplitude of the first excited state (S_1) absorption peak (ESA) in a spectral region, particularly at early probe delay times, that is free of contributions from other

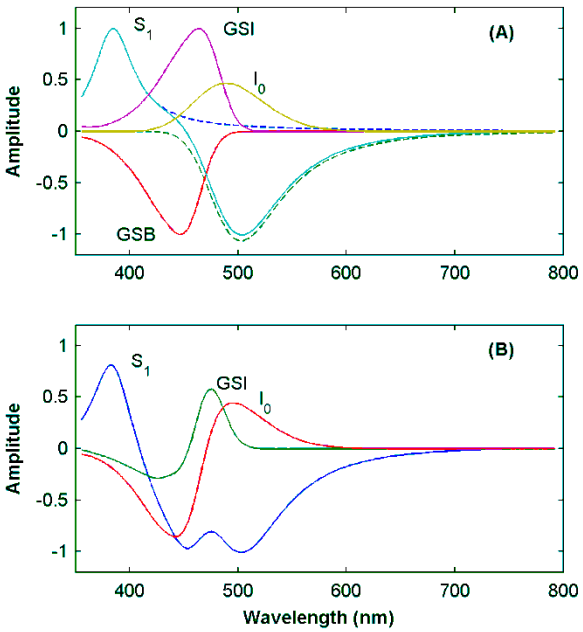

Fig. S1 A) State-associated spectrum of GSB, S_1, GSI and I0, initialisation for target fitting (solid curves). Dashed curves are the excited state absorption and stimulated emission spectra underlying the S_1 spectrum. B) SADS calculated by addition of the GSB spectra to each remaining spectra.

states (see Figs. 2 and 3 and reference [2] for example). The second wavelength of 670 nm corresponds to the peak absorption amplitude of a hydrated electron state in a spectral region clear of contributions from other states particularly at longer delays (Figs. 2 and 3for example). The hydrated electron is produced through ionisation of the PYP chromophore via excitation into a second excited state (S_2) via stepwise multi-photon process as previously proposed.[2] The power-dependent transient absorption data were then decomposed using the *mldivide* function and the power-dependent concentration curves into one- and multi-photon dependent spectra. This process was repeated for all probe delay times resulting in time-dependent datasets. These were normalised at 446 nm, the same scaling factor was then used to rescale the power-dependent concentration curves (Fig. 3).

Target analysis was performed in two steps. The first was to fit state-associated spectra to the transient absorption data to extract time-dependent state-associated concentration traces (TD-SACT). The fit was initialised with idealised state-associated lineshapes, (Fig. S1) and a set of TD-SACT was retrieved from the transient absorption spectra using the *mldivide* function. The state-associated spectra were ground state bleach (GSB), stimulated emission (SE) and excited state absorption (ESA) as a single excited state (S_1), ground state intermediate (GSI) and the

primary photocycle product (I_0), see Fig. S1. The GSB was modelled as PYP steady-state absorption with an amplitude fixed to -1. Fixing the GSB minimum amplitude to -1 was essential for keeping the remaining spectra correctly scaled. The SE was modelled by spectral shifting and broadening (with free parameters) a PYP fluorescence spectrum taken from ref [3]. The ESA was modelled as Voigt function (calculated by convolution of a Gaussian with a Lorentzian) with fixed positive amplitude of 1, the centre wavelength and Gaussian/Lorentzian widths were free parameters. S_1 was taken as the sum of the SE and ESA spectra. The initial idealised lineshape of SE was shifted from 495 nm to near 500 nm and broadened from 47 nm (FWHM) to 76 nm (FWHM). The ESA was initialised with a centre wavelength of 386 nm a width of 57 nm (FWHM) (Fig. S1). The GSI was modelled as a spectrally shifted (free parameter) ground-state absorption spectrum. The initial idealised lineshape was shifted 17 nm to the red relative to the GSB. Finally, the I_0 spectrum was modelled using a Voigt centred at 489 nm and width of 82 nm (FWHM), which modelled the long delay spectral differences well, as shown previously.[2, 4] The amplitude and Gaussian and Lorentzian widths were free parameters. The state-associated difference spectra (SADS) shown in figure S1 are in reasonable agreement with the observed transient absorption spectra for PYP and those found previously,[2, 4] and which biases the fitting to those models. The TD-SACT, excluding the GSB component, were then applied to the transient absorption data and the SADS retrieve using the *mldivide* function. This process was repeated in a minimisation routine that satisfied the conditions that i) the GSB concentration trace was always decaying, i.e., minimising any increasing concentration, ii) the sum of the remaining concentration traces was equal to the GSB curve, iii) none of the concentration traces could have negative values, and iv) minimised the difference between calculated (Fig. S1) and retrieved SADS. The fits were performed simultaneously on all *n* transient absorption spectra measured at *n* different excitation powers. The final SADS and TD-SACT were then used to fit a target model.

The target model is described by a series of coupled differential equations (Eq. S1a-h and Fig. 1) that calculates the rates for stimulated process using photoselection theory to account for photoselection of the magic angle probe and the excitation power and pulse duration dependence of the stimulated absorption (SA) and stimulated emission (SE) of S_1 and S_2.

$$\frac{d[S_0]}{dt} = -\boldsymbol{k}_{01s}(t)[S_0] + \boldsymbol{k}_{10s}(t)[S_1^0] + \varphi_{S_1^0\to S_0}\boldsymbol{k}_{s_1^0}[S_1^0] + \varphi_{S_1^1\to S_0}\boldsymbol{k}_{s_1^1}[S_1^1] + \varphi_{S_1^2\to S_0}\boldsymbol{k}_{s_1^2}[S_1^2] + \boldsymbol{k}_{s_{GSI}}[S_{GSI}] + \varphi_{S_2\to S_1}\boldsymbol{k}_{S_2}[S_2] \quad \text{(S1a)}$$

$$\frac{d[S_1^0]}{dt} = \boldsymbol{k}_{01s}(t)[S_0] - \boldsymbol{k}_{10s}(t)[S_1^0] - \boldsymbol{k}_{12s}(t)[S_1^0] + \boldsymbol{k}_{21s}(t)[S_2] - \varphi_{S_1^0\to S_1^1}\boldsymbol{k}_{s_1^0}[S_1^0] - \varphi_{S_1^0\to I_0}\boldsymbol{k}_{s_1^0}[S_1^0] - \varphi_{S_1^0\to S_{GSI}}\boldsymbol{k}_{s_1^0}[S_1^0] - \varphi_{S_1^0\to S_0}\boldsymbol{k}_{s_1^0}[S_1^0] \quad \text{(S1b)}$$

$$\frac{d[S_1^1]}{dt} = \varphi_{S_1^0\to S_1^1}\boldsymbol{k}_{s_1^0}[S_1^0] - \varphi_{S_1^1\to S_1^2}\boldsymbol{k}_{s_1^1}[S_1^1] - \varphi_{S_1^1\to I_0}\boldsymbol{k}_{s_1^1}[S_1^1] - \varphi_{S_1^1\to S_{GSI}}\boldsymbol{k}_{s_1^1}[S_1^1] - \varphi_{S_1^1\to S_0}\boldsymbol{k}_{s_1^1}[S_1^1] \quad \text{(S1c)}$$

$$\frac{d[S_1^2]}{dt} = \varphi_{S_1^1\to S_1^2}\boldsymbol{k}_{s_1^1}[S_1^1] - \varphi_{S_1^2\to I_0}\boldsymbol{k}_{s_1^2}[S_1^2] - \varphi_{S_1^2\to S_{GSI}}\boldsymbol{k}_{s_1^2}[S_1^2] - \varphi_{S_1^2\to S_0}\boldsymbol{k}_{s_1^2}[S_1^2] \quad \text{(S1d)}$$

$$\frac{d[I_0]}{dt} = \varphi_{S_1^0\to I_0}\boldsymbol{k}_{s_1^0}[S_1^0] + \varphi_{S_1^1\to I_0}\boldsymbol{k}_{s_1^1}[S_1^1] + \varphi_{S_1^2\to I_0}\boldsymbol{k}_{s_1^2}[S_1^2] - \boldsymbol{k}_{I_0}[I_0] \quad \text{(S1e)}$$

$$\frac{d[S_{GSI}]}{dt} = \varphi_{S_1^0\to S_{GSI}}\boldsymbol{k}_{s_1^0}[S_1^0] + \varphi_{S_1^1\to S_{GSI}}\boldsymbol{k}_{s_1^1}[S_1^1] + \varphi_{S_1^2\to S_{GSI}}\boldsymbol{k}_{s_1^2}[S_1^2] - \boldsymbol{k}_{S_{GSI}}[S_{GSI}] \quad \text{(S1f)}$$

$$\frac{d[S_2]}{dt} = \boldsymbol{k}_{12s}(t)[S_1] - \boldsymbol{k}_{21s}(t)[S_2] - \varphi_{S_2\to e^-}\boldsymbol{k}_{S_2}[S_2] - \varphi_{S_2\to S_0}\boldsymbol{k}_{S_2}[S_2] \quad \text{(S1g)}$$

$$\frac{d[e^-]}{dt} = \varphi_{S_2\to e^-}\boldsymbol{k}_{S_2}[S_2] \quad \text{(S1h)}$$

where, S_0 is the electronic ground state, S_1^i are the *i*th intermediates of the first excited state and S_2 is the second electronic excited state; e^- represents all states created via S_2, i.e., the hydrated electron and radical pair as well as the other intermediates; I_0 is the primary photocycle product and S_{GSI} is the ground state intermediate. $\boldsymbol{k}_{Si}$, $\boldsymbol{k}_{Io}$ and $\boldsymbol{k}_{GSI}$ are the corresponding relaxation rates. $\varphi_{x\to y}$ represent the branching yields for relaxation between states *x* and *y*. Finally, $\boldsymbol{k}_{ijs}(t)$ are the rates of stimulated absorption (*ij*) or emission (*ji*) between states *ij* calculated using photoselection theory taking into account the effect of polarisation which allows for the retrieval of the corresponding cross-sections and quantum yields as follows:

$$\boldsymbol{k}_{ijs}(t) = 3J(t)\,\sigma_{ij}\,\Phi_{ij}\cos^2\theta$$

and,

$$\sigma_{ij} = \frac{1000\times\ln(10)\times\boldsymbol{\varepsilon}_{ijs}}{N_A}$$

where, $J(t)$ is a Gaussian profile of photon flux as a function of time (Gaussian profile of photons/cm/s), σ_{ij} the absorption/stimulated emission cross-sections with units cm^2/molecule, ε_{ijs} are the absorption or stimulated emission Molar extinction coefficients with units $M^{-1}cm^{-1}$ and Φ_{ij} are the quantum yields, for transitions between electronic states (*i* to *j*) or (*j* to *i*), respectively, θ is the angle of polarisation relative to the pump and N_A is Avogadro's number with units molecule/mol. Equations 1a-h were solved numerically in the Matlab environment using a time step *dt* of 5 fs.

Fits were performed simultaneously on all *n* transient absorption spectra measured at *n* different excitation powers to retrieve the absorption/emission cross-sections, quantum yield for S_1 formation, and branching yields and decay rates for all relaxation processes. Fixed parameters were the ground state cross-sections (6.31×10^{-17}, 1.68×10^{-16} and 1.26×10^{-17} cm^2/molecule for 400, 450 and 490 nm excitation wavelengths), quantum yields for S_1 absorption and emission and S_2 emission were set to 1; θ was fixed at 54.7° to account for the magic angle probe and the decay rate of the third excited state intermediate S_1^2 to 40 ps.

For 400 nm excitation the sample was also optically 'thick' meaning the sample concentration and ground state absorption cross-section were sufficiently high to absorb a significant

number of photons within the sample length. To account for this the above numerical fit of equations S1a-h were repeated with flux $J(t) = Jo(t)\ x10^{-\alpha z}$, where $J0(t)$ was the initial flux, α the linear absorption at the pump wavelength and $z = zi/l$ the normalised penetration depth zi to sample length l. The final state dependent concentrations [S's] were taken as the average over the number of zi penetration depths used in the calculation.

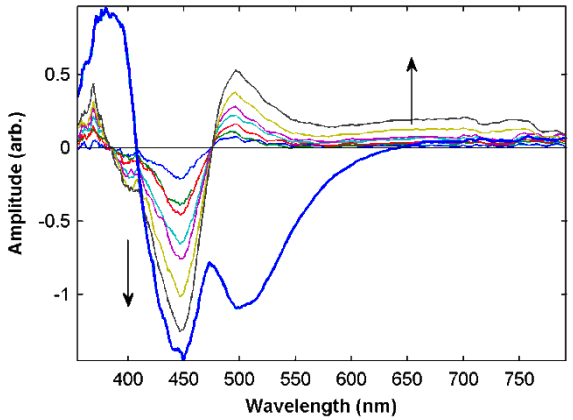

Fig. S2 Difference transient absorption spectra of PYP excited with 400 nm, 300 fs pulse duration and eight different powers at a probe delay of 0.4 ps and normalised at 386 nm (Thin lines). For reference the lowest excitation power transient absorption spectra is included with arbitrary scaling (Thick line). Arrows indicate increasing excitation power.

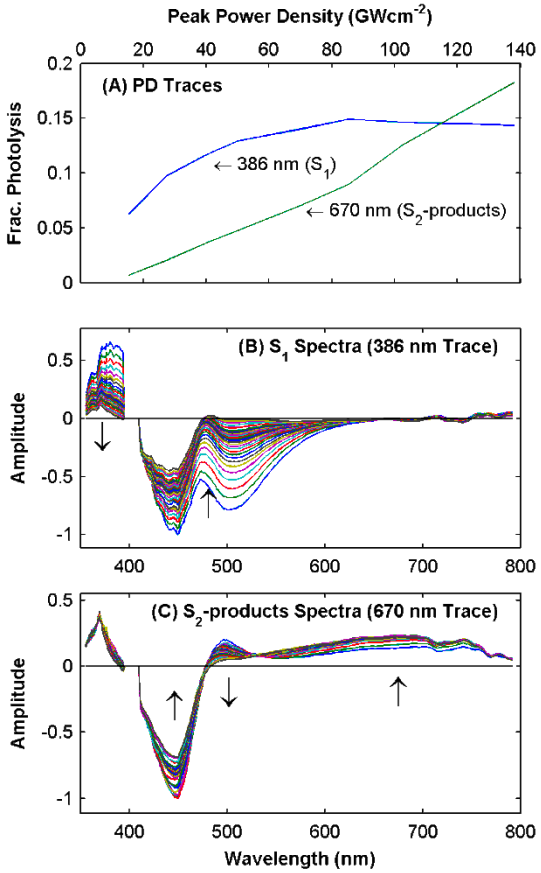

Fig. S3 PYP excited at 400nm and 300 fs pulse duration. A) Power-dependent concentration profiles taken from the maximum amplitudes of the TA spectra at wavelengths 386 and 670 nm that correspond to the ESA (S_1) and hydrated electron (S_2-products) states. These power-dependent concentration curves were then used to decompose the power-dependent (PD) spectra at each time delay into S_1 and S_2-products contributions (panels B and C); arrows indicate increasing time delay.

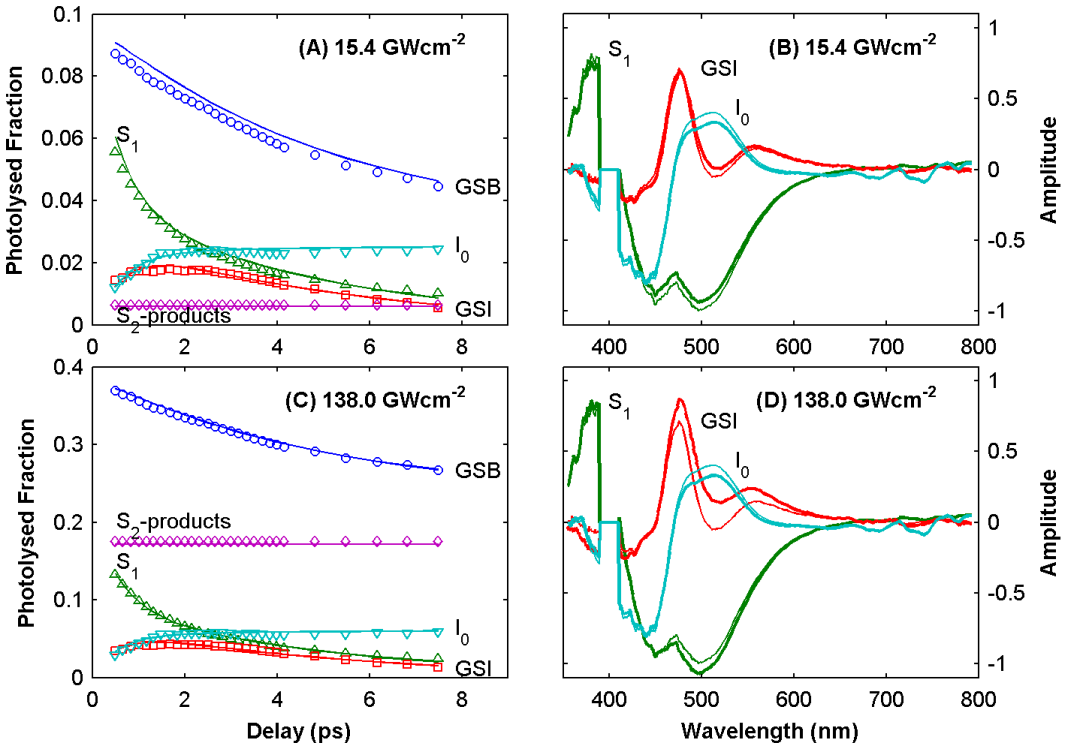

Fig. S4 Target analysis of PYP excited with 400 nm, 300 fs pulses. Panels A and C show the TD-SACT for GSB, S_1, GSI, I_0 and S_2-products (circles, upward triangles, squares and downward triangles, diamonds) for the lowest and highest excitation powers (15.4 and 138 GWcm^{-2}). Panels B and C show the corresponding SADS used to generate the TD-SACT (Thin lines). Panels A and C solid lines and panels B and D thick lines, results of a global target fitting using the model described by equations S1a-h and parameters table 1.

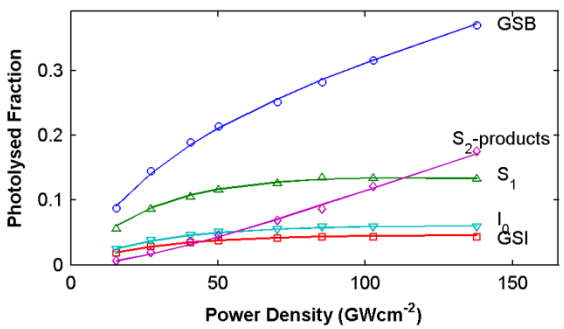

Fig. S5 TD-SACT maxima as function of power-dependence for GSB, S_1, GSI, I_0 and S_2-products (circles, upward triangle, squares, downward triangles and diamonds) results of target analysis of PYP excited at 400 nm, 300 fs pulses of eight different powers.

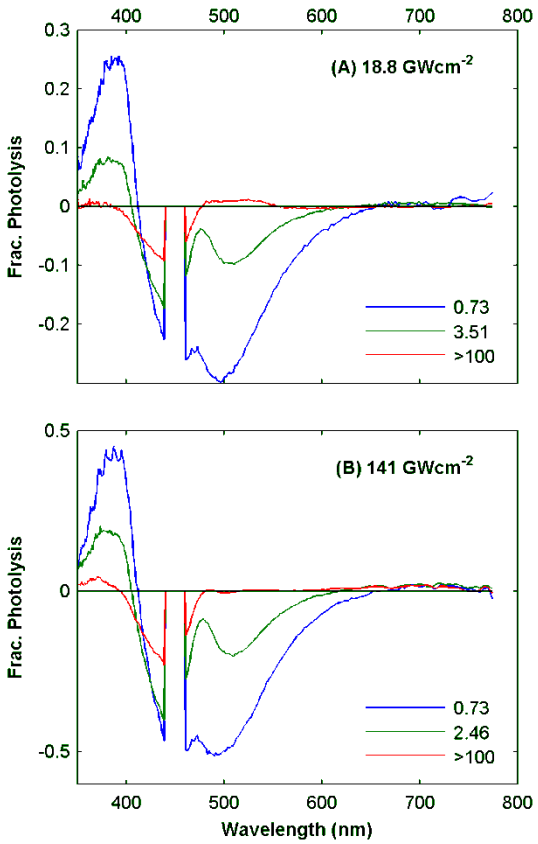

Fig. S6 Fitted EADS using a three state sequential model of; A) the lowest (18.8 $GWcm^{-2}$) and B) highest (141 $GWcm^{-2}$) power density TA spectra of PYP excited 450 nm and 140 fs pulses. The lifetime of the three states are indicated in ps. Note the lifetime of the third state was fixed to 200 ps.

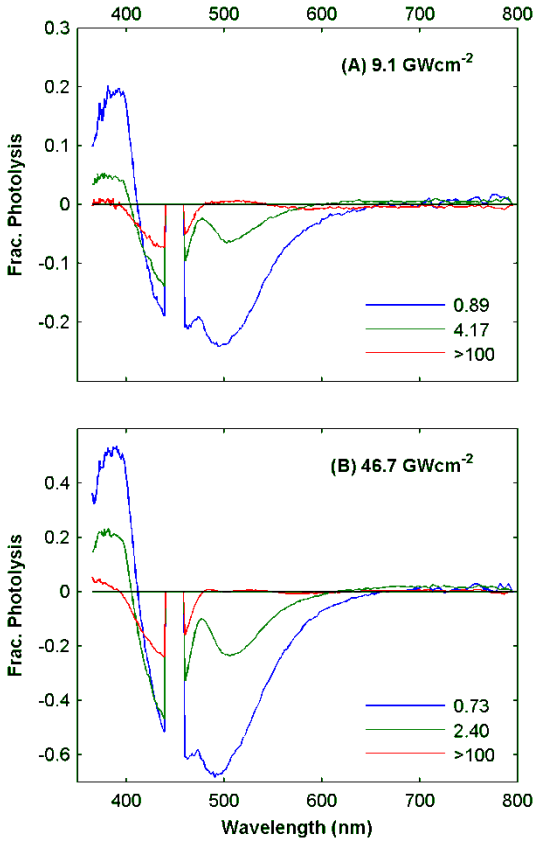

Fig. S7 Fitted EADS using a three state sequential model of; A) the lowest (9.1 $GWcm^{-2}$) and B) highest (46.7 $GWcm^{-2}$) power density TA spectra of PYP excited 450 nm and 300 fs pulses. The lifetime of the three states are indicated in ps. Note the lifetime of the third state was fixed to 200 ps.

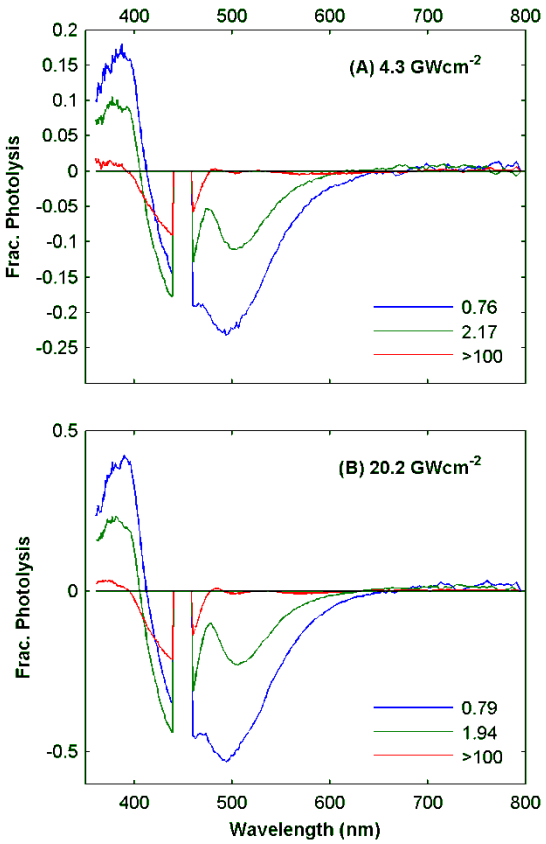

Fig. S8 Fitted EADS using a three state sequential model of; A) the lowest (4.3 $GWcm^{-2}$) and B) highest (20.2 $GWcm^{-2}$) power density TA spectra of PYP excited 450 nm and 600 fs pulses. The lifetime of the three states are indicated in ps. Note the lifetime of the third state was fixed to 200 ps.

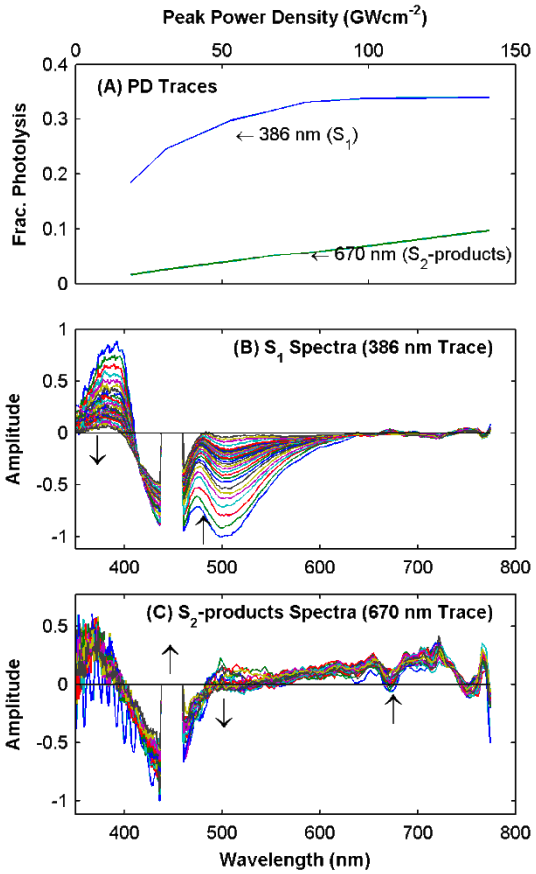

Fig. S9 PYP excited with 450 and 140 fs pulses. A) Power-dependent concentration profiles taken from the maximum amplitudes of the PYP TA spectra at wavelengths 386 and 670 nm that correspond to the ESA (S_1) and hydrated electron (S_2-products) states. These power-dependent concentration curves were then used to decompose the power-dependent (PD) spectra at each time delay into S_1 and S_2-products contributions (panels B and C). B and C) arrows indicate increasing time delay.

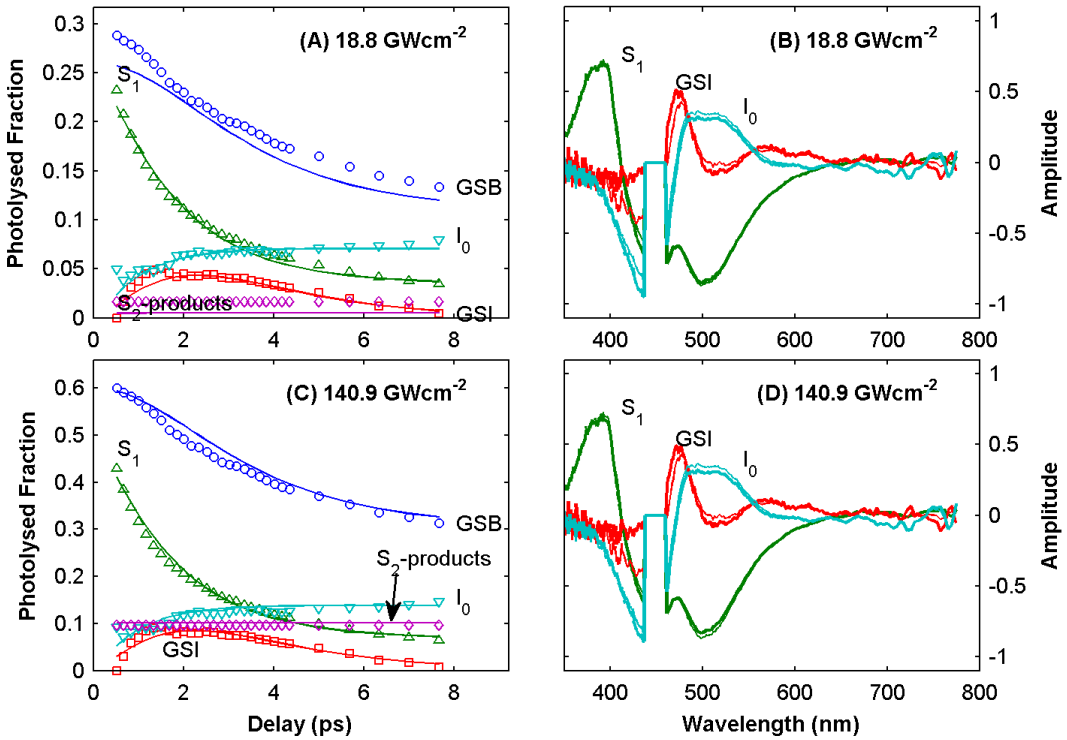

Fig. S10 Target analysis of PYP excited with 450 nm, 140 fs pulses. Panels A and C show TD-SACT for GSB, S_1, GSI, I_0 and S_2-products (circles, upward triangles, squares and downward triangles, diamonds) for the lowest and highest excitation power (18.8 and 141 GWcm^{-2}). Panels B and C show the corresponding SADS used to generate the TD-SCAT (Thin lines). Panels A and C solid lines and panels B and D thick lines, results of a global target fitting using the model described by equations S1a-h and parameters table 2.

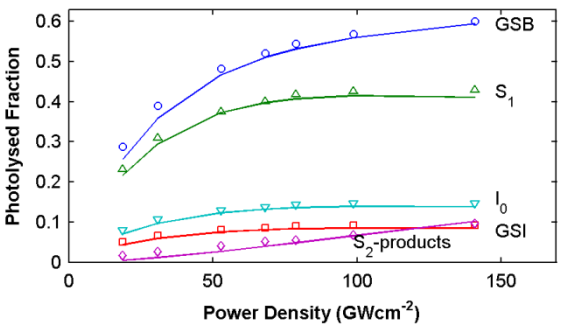

Fig. S11 TD-SACT maxima as function of power-dependence for GSB, S_1, GSI, I_0 and S_2-products (circles, upward triangle, squares, downward triangles and diamonds) results of target analysis of PYP excited at 450 nm, 140 fs pulses of seven different powers.

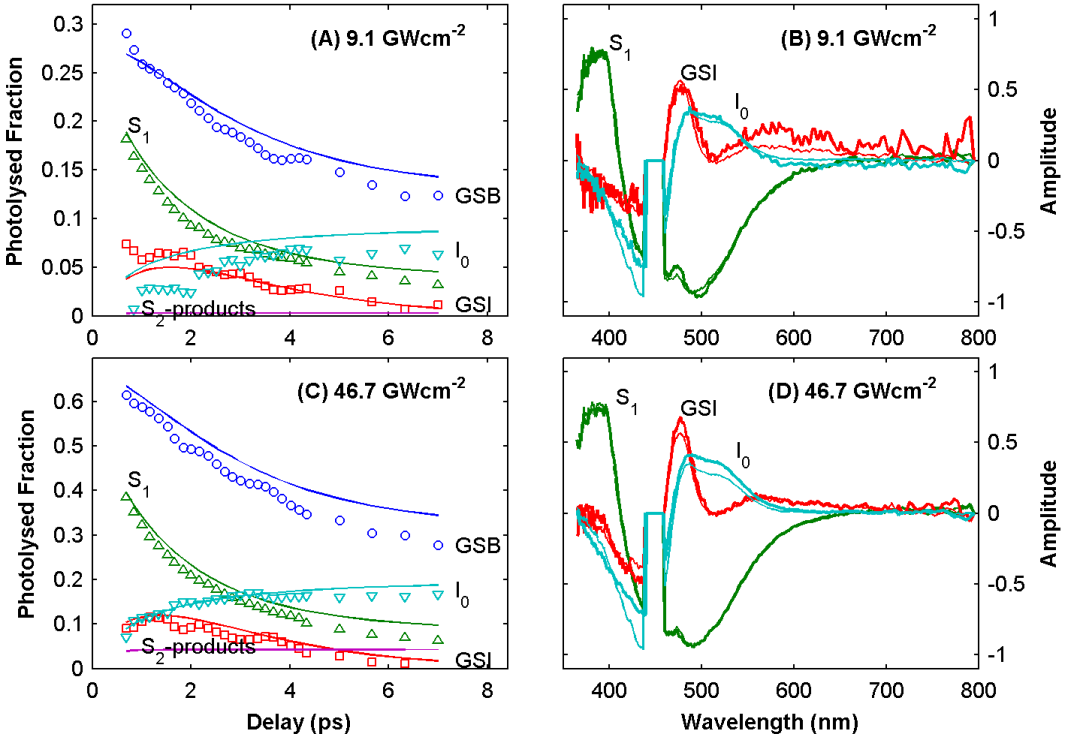

Fig. S12 Target analysis of PYP excited with 450 nm, 300 fs pulses. Panels A and C show TD-SACT for GSB, S_1, GSI, I_0 and S_2 (circles, upward triangles, squares and downward triangles, diamonds) for the lowest and highest excitation power (9.1 and 46.7 $GWcm^{-2}$). Panels B and C show the corresponding SADS used to generate the TD-SACT (Thin lines). Panels A and C solid lines and panels B and D thick lines, results of a global target fitting using the model described by equations S1a-h and parameters table S1.

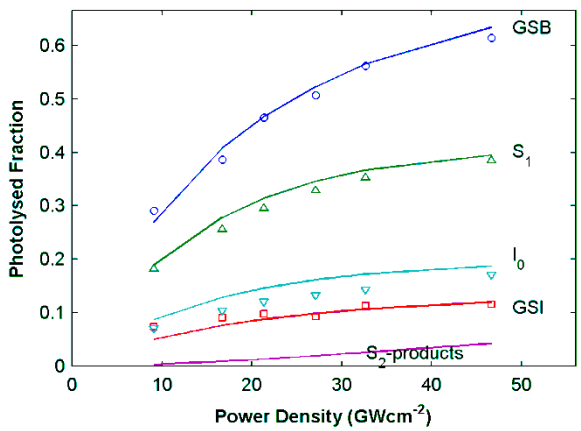

Fig. S13 TD-SACT maxima as function of power-dependence for GSB, S_1, GSI, I_0 and S_2–products (circles, upward triangle, squares, downward triangles and diamonds) results of target analysis of PYP excited at 450 nm, 300 fs pulses of six different powers.

Table S1 Fitting parameters for target analysis of PYP excited with 450 nm and 300 fs pulses. σ_{ijs} are the absorption and emission cross sections for transition between S_0 and S_1 (ij = 01 and 10) and S_1 and S_2 (ij = 12 and 21). The quantum yield for ground state absorption is 0.52. Branching yields into states GSB, GSI, I_0 and S_1^{i+1} are listed in columns for each excited state intermediate S_1^i (i = 0,1,2) for relaxation into the ground state, ground state intermediate, the primary photocycle product and the next excited state intermediate, respectively. The lifetimes (1/ks) are 0.4, 1.7, 40.0 ps for excited state intermediates (S_1^i (i = 0,1,2)), 1.5 ps for GSI and 30 fs for S_2. The branching yields for S_2 relaxation to e^- and S_1^0 were 0.57 and 0.43, respectively.

Cross-section x10^{-16} (cm^2/molecule)			
σ_{01s}	σ_{10s}	σ_{12s}	σ_{21s}
1.68	0.704	0.117	0.00
Branching Yields			
States	S_1^0	S_1^1	S_1^2
GSB	0.00	0.02	0.18
GSI	0.13	0.52	0.08
I_0	0.15	0.22	0.74
S_1^{i+1}	0.72	0.24	-

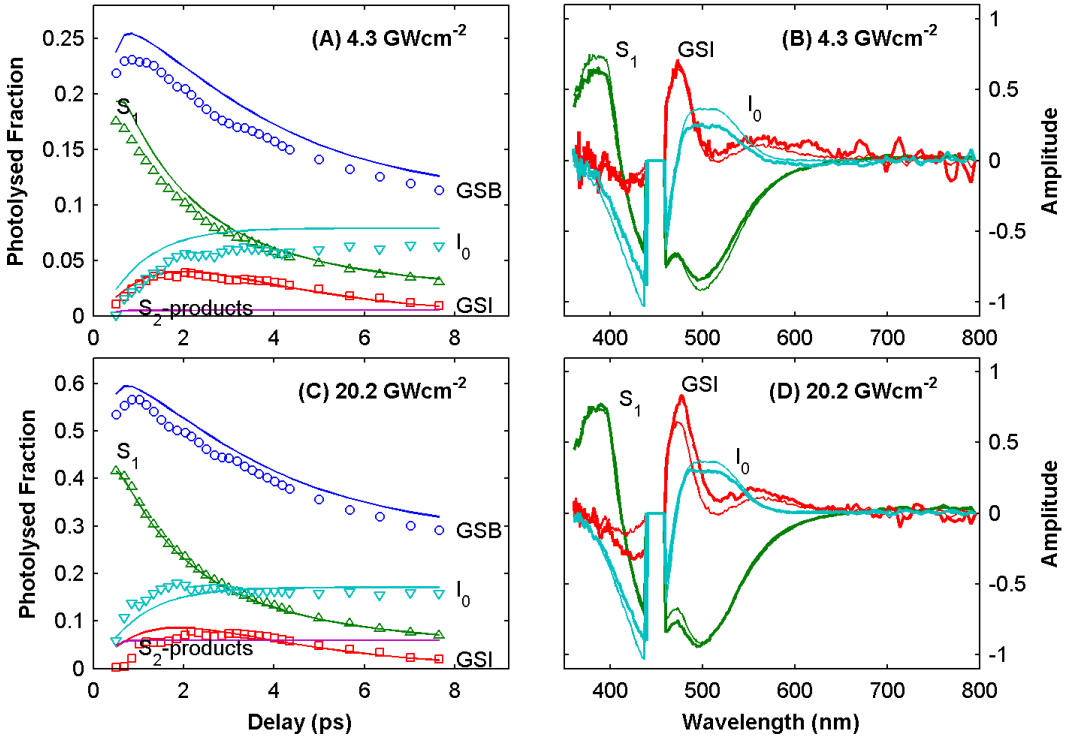

Fig. S14 Target analysis of PYP excited with 450 nm, 600 fs pulses. Panels A and C show TD-SACT for GSB, S_1, GSI, I_0 and S_2–products (circles, upward triangles, squares and downward triangles, diamonds) for the lowest and highest excitation power (9.1 and 46.7 GWcm^{-2}). Panels B and C show the corresponding SADS used to generate the TD-SACT (Thin lines). Panels A and C solid lines and panels B and D thick lines, results of a global target fitting using the model described by equations S1a-h and parameters table S2.

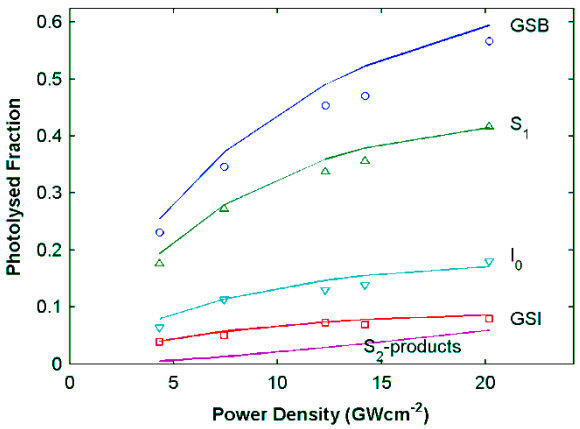

Fig. S15 TD-SACT maxima as function of power-dependence for GSB, S_1, GSI, I_0 and S_2–products (circles, upward triangle, squares, downward triangles and diamonds) results of target analysis of PYP excited at 450 nm, 600 fs pulses of five different powers.

Table S2 Fitting parameters for target analysis of PYP excited with 450 nm and 600 fs pulses. σ_{ijs} are the absorption and emission cross sections for transition between S_0 and S_1 (ij = 01 and 10) and S_1 and S_2 (ij = 12 and 21). The quantum yield for ground state absorption is 0.52. Branching yields into states GSB, GSI, I_0 and S_1^{i+1} are listed in columns for each excited state intermediate S_1^i (i = 0,1,2) for relaxation into the ground state, ground state intermediate, the primary photocycle product and the next excited state intermediate, respectively. The lifetimes (1/ks) are 0.9, 2.5, 40.0 ps for excited state intermediates (S_1^i (i = 0,1,2)), 1.5 ps for GSI and 30 fs for S_2. The branching yields for S_2 relaxation to e^- and S_1^0 were 0.59 and 0.41, respectively.

Cross-section x10^{-16} (cm^2/molecule)			
σ_{01s}	σ_{10s}	σ_{12s}	σ_{21s}
1.68	0.681	0.117	0.00
Branching Yields			
States	S_1^0	S_1^1	S_1^2
GSB	0.00	0.07	0.73
GSI	0.22	0.70	0.27
I_0	0.31	0.00	0.00
S_1^{i+1}	0.48	0.24	-

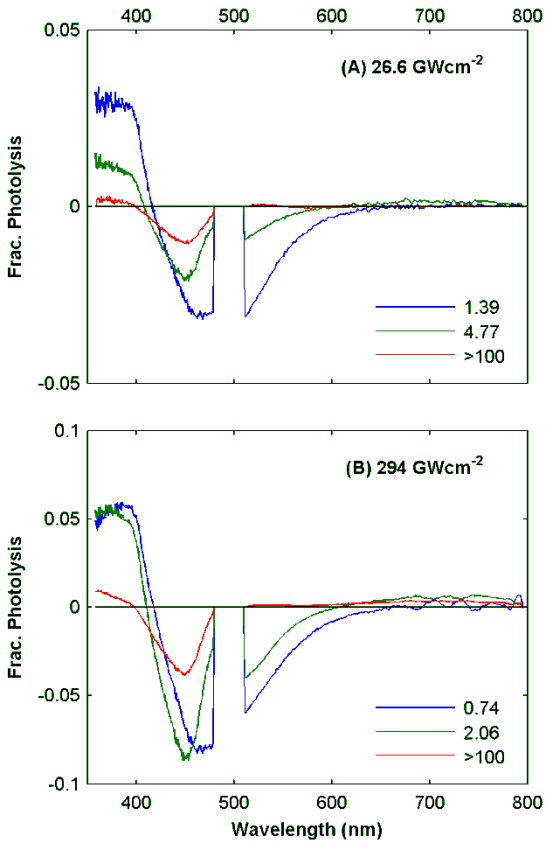

Fig. S16 Fitted EADS using a three state sequential model of; A) the lowest (26.6 $GWcm^{-2}$) and B) highest (294 $GWcm^{-2}$) power density TA spectra of PYP excited 490 nm and 300 fs pulses. The associated time constants of the three states are indicated in ps. Note the time constant of the third state was fixed to 200 ps.

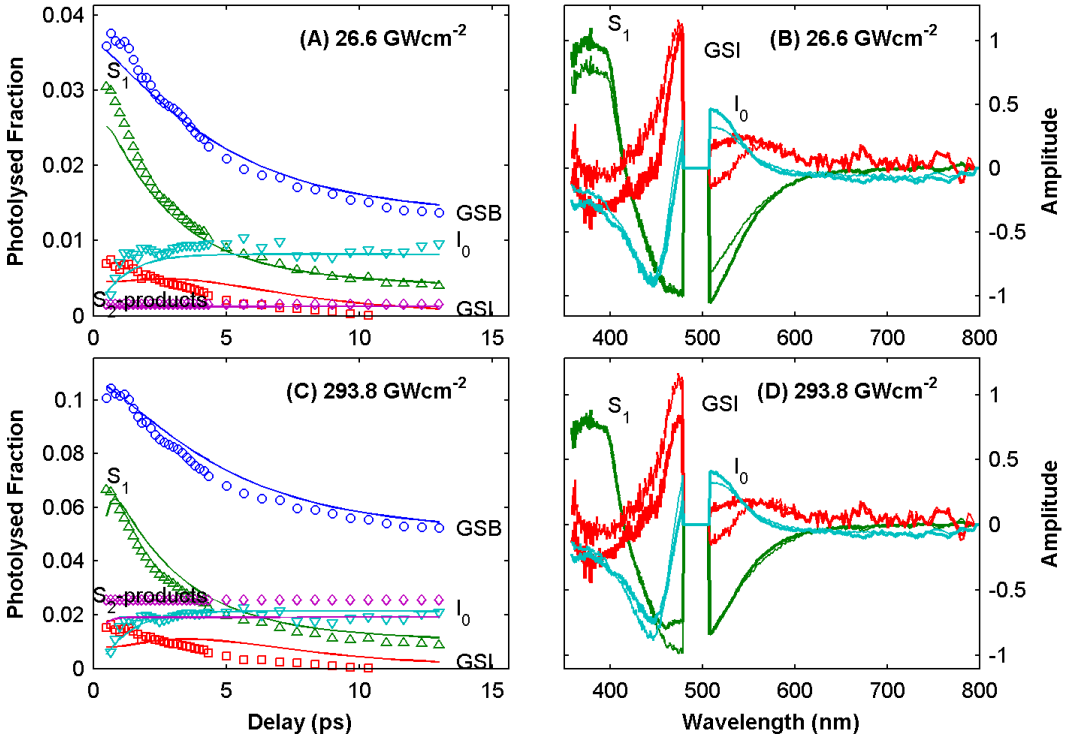

Fig. S17 Target analysis of PYP excited with 490 nm, 300 fs pulses. Panels A and C show TD-SACT for GSB, S_1, GSI, I_0 and S_2-products (circles, upward triangles, squares and downward triangles, diamonds) for the lowest and highest excitation power (18.8 and 141 GWcm^{-2}). Panels B and C show the corresponding SADS used to generate the TD-SACT (Thin lines). Panels A and C solid lines and panels B and D thick lines, results of a global target fitting using the model described by equations S1a-h and parameters table 3.

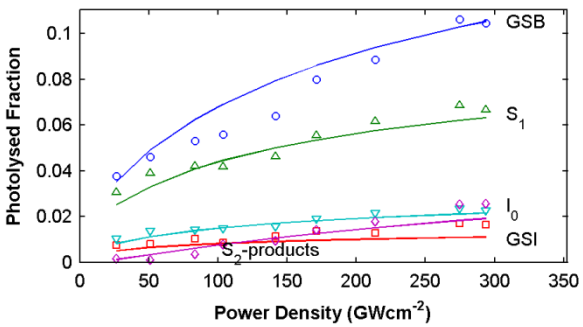

Fig. S18 TD-SACT maxima as function of power-dependence for GSB, S_1, GSI, I_0 and S_2-products (circles, upward triangle, squares, downward triangles and diamonds) results of target analysis of PYP excited at 490 nm, 300 fs pulses of nine different powers.

References

1. L. J. van Wilderen, C. N. Lincoln and J. J. van Thor, *PLoS One*, 2011, **6**, e17373.
2. D. S. Larsen, I. H. van Stokkum, M. Vengris, M. A. van Der Horst, F. L. de Weerd, K. J. Hellingwerf and R. van Grondelle, *Biophys J*, 2004, **87**, 1858-1872.
3. T. E. Meyer, G. Tollin, T. P. Causgrove, P. Cheng and R. E. Blankenship, *Biophys J*, 1991, **59**, 988-991.
4. A. D. Stahl, M. Hospes, K. Singhal, I. van Stokkum, R. van Grondelle, M. L. Groot and K. J. Hellingwerf, *Biophys J*, 2011, **101**, 1184-1192.

Singular Value Decomposition

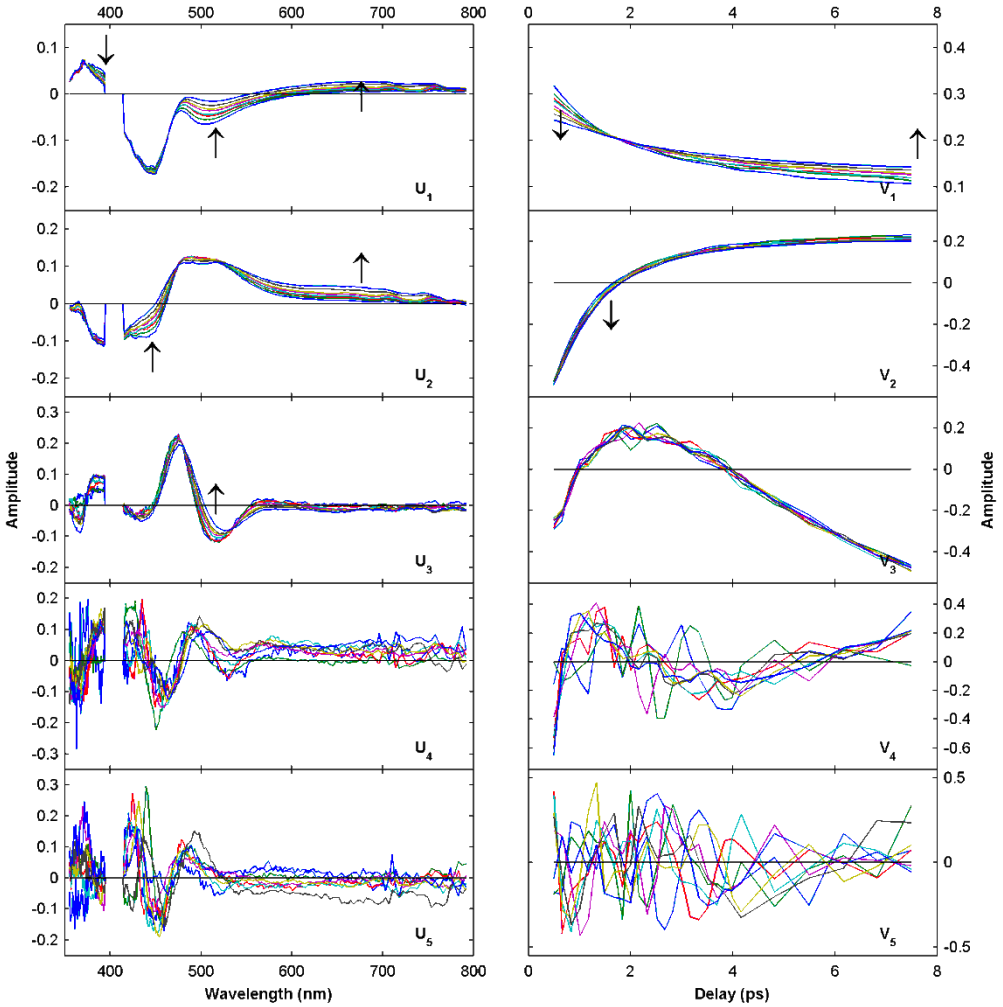

Fig. S19 SVD results of time-dependent transient absorption spectra of PYP excited with 400 nm, 300 fs pulses at eight different excitation powers. The fit was applied only to delays greater than 0.4 ps to avoid the early time coherent artefact. Plotted are the left (U_i) and right (V_i) singular vectors for the first five singular values for each excitation power (arrows indicate increasing power). For clarity the singular values are plotted separately (Fig. S20). They are for the lowest power (15.4 GWcm^{-2}) 1.600, 0.340, 0.032, 0.008, 0.008 and the highest power (138 GWcm^{-2}) 7.647, 1.015, 0.135, 0.040, 0.019.

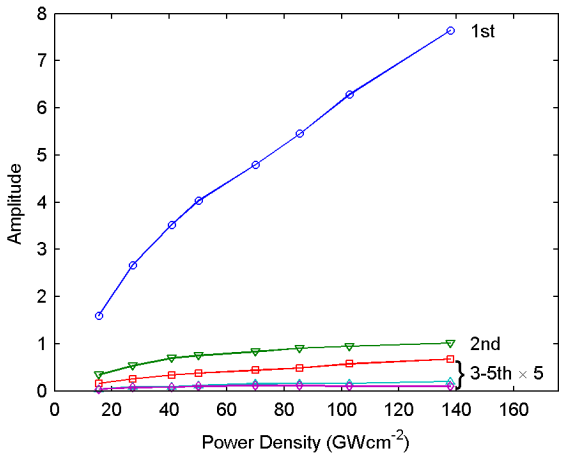

Fig. S20 First 5 singular values of SVD analysis of time-dependent transient absorption spectra of PYP excited at 400 nm and 300 fs pulses plotted against the eight different excitation powers, see figure S19 for more detail. Note solid lines are included to guide the eye.

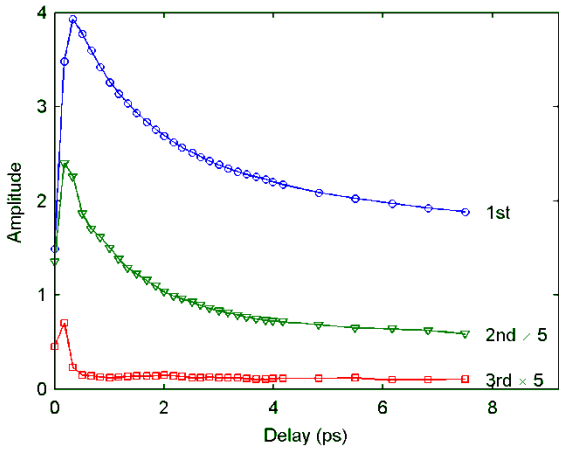

Fig. S21 First three singular values of SVD analysis of power-dependent transient absorption spectra of PYP excited at 400 nm and 300 fs plotted against each measured delay time, see figure S22 for details. Note solid lines are included to guide the eye.

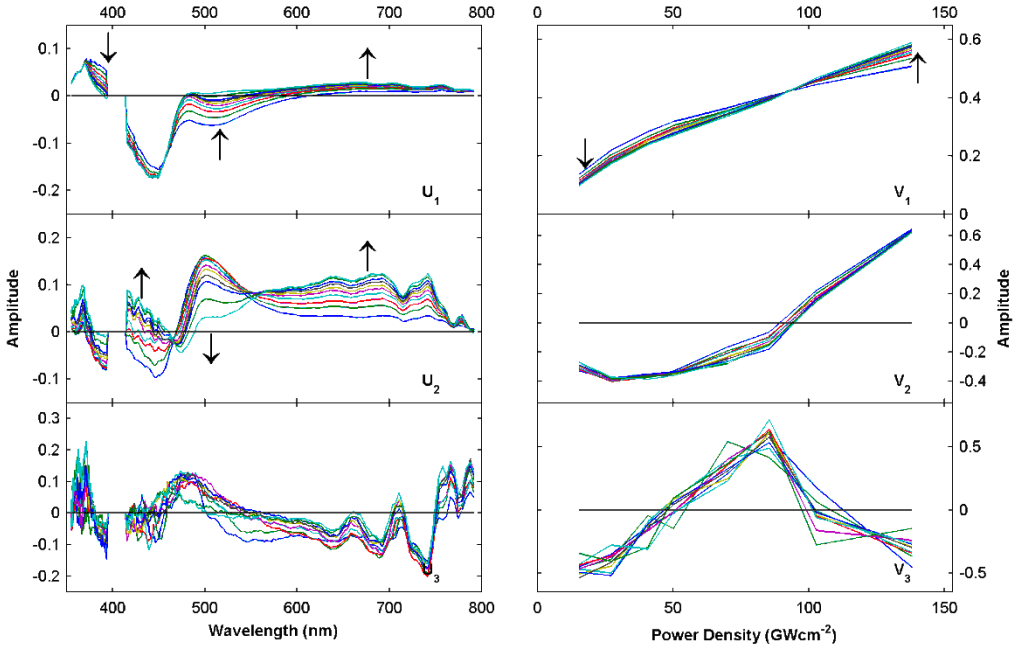

Fig. S22 Results of SVD of power-dependent transient absorption spectra of PYP excited with 400 nm, 300 fs and ten time delays between 0.4 and 7.5 ps. Plotted are the left (U_i) and right (V_i) singular vectors for the first three singular values (arrows indicate increasing probe delay time). For clarity the singular values are plotted separately (Fig. S21). The singular values are 3.774, 0.372, 0.0291 (0.5 ps delay) and 1.884, 0.117, 0.022 (7.5 ps delay).

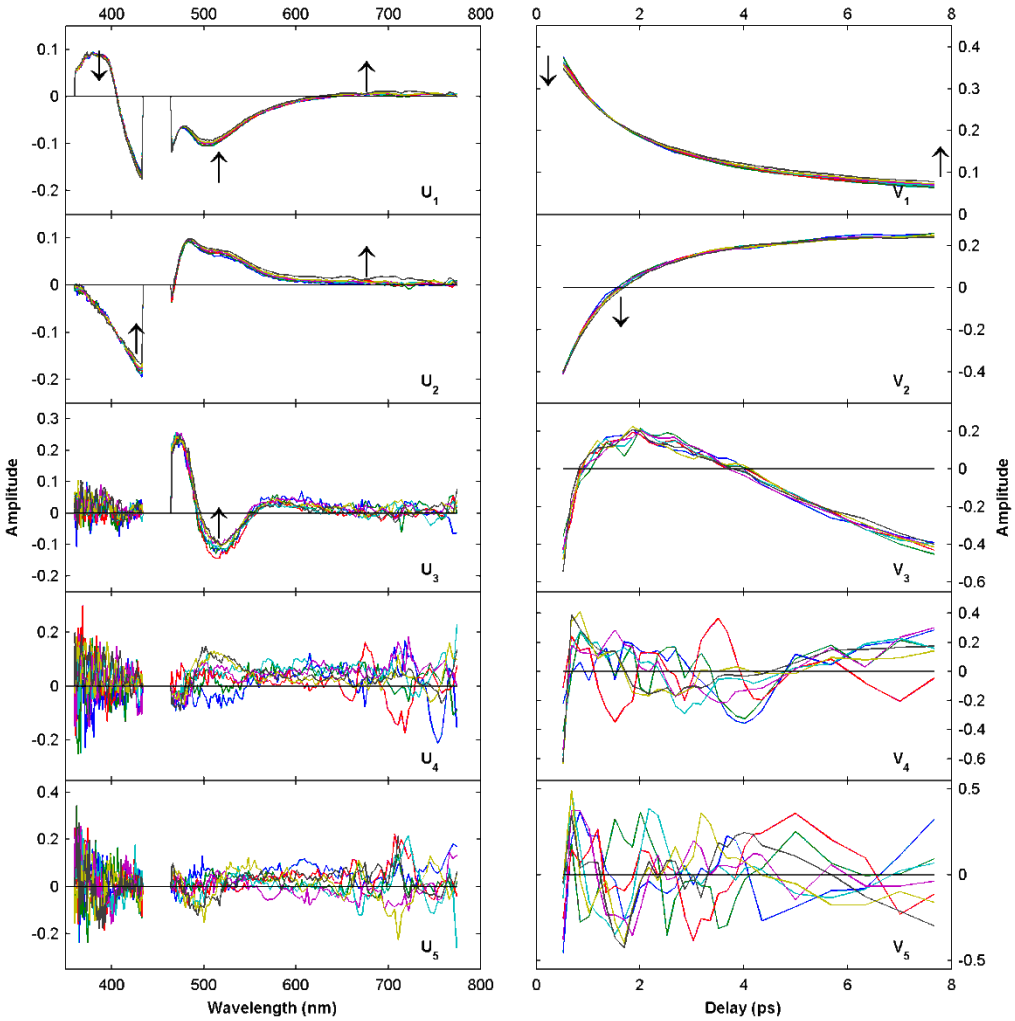

Fig. S23 SVD results of time-dependent transient absorption spectra of PYP excited with 450 nm, 140 fs pulses at seven different excitation powers. The fit was applied only to delays greater than 0.4 ps to avoid early time artefact. Plotted are the left (U_i) and right (V_i) singular vectors for the first five singular values for each excitation power (arrows indicate increasing power). For clarity the singular values are plotted separately (Fig. S24). They are for the lowest power (18.8 $GWcm^{-2}$) 4.03, 1.01, 0.104, 0.050, 0.045 and the highest power (141 $GWcm^{-2}$) 8.150, 2.108, 0.189, 0.111, 0.054.

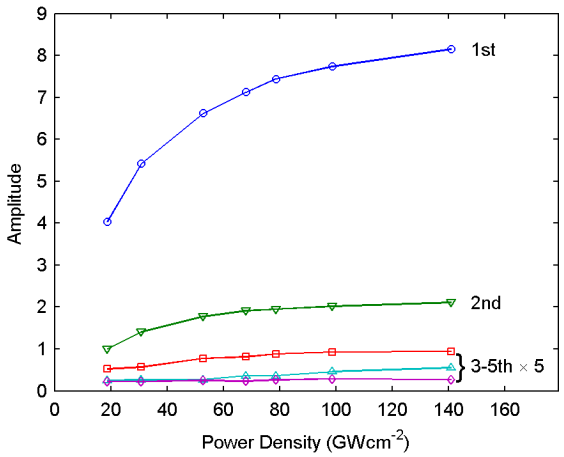

Fig. S24 First 5 singular values from SVD decomposition of time-dependent transient absorption spectra of PYP excited at 450 nm and 140 fs pulses plotted against the seven different excitation powers, see figure S23 for more detail.

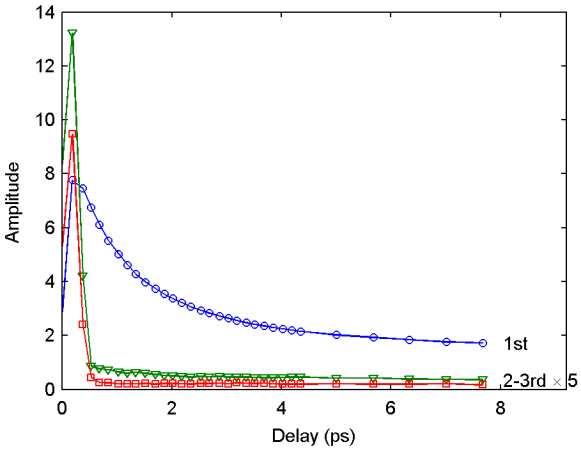

Fig. S25 First three singular values of SVD analysis of power-dependent transient absorption spectra of PYP excited at 450 nm and 140 fs plotted against each measured delay time, see figure S26 for details.

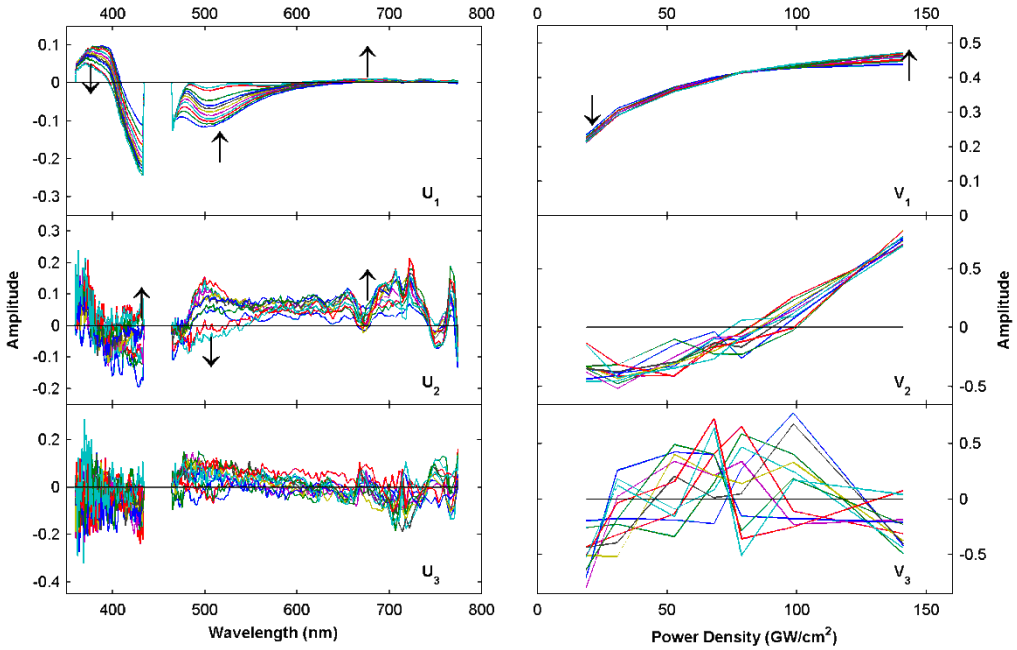

Fig. S26 Results of SVD of power-dependent transient absorption spectra of PYP excited with 450 nm, 140 fs and ten time delays between 0.4 and 7.5 ps. Plotted are the left (U_i) and right (V_i) singular vectors for the first three singular values (arrows indicate increasing probe delay time). For clarity the singular values are plotted separately (Fig. S25). The singular values are 6.74, 0.172, 0.088 (0.5 ps delay) and 1.723, 0.073, 0.035 (7.5 ps delay).

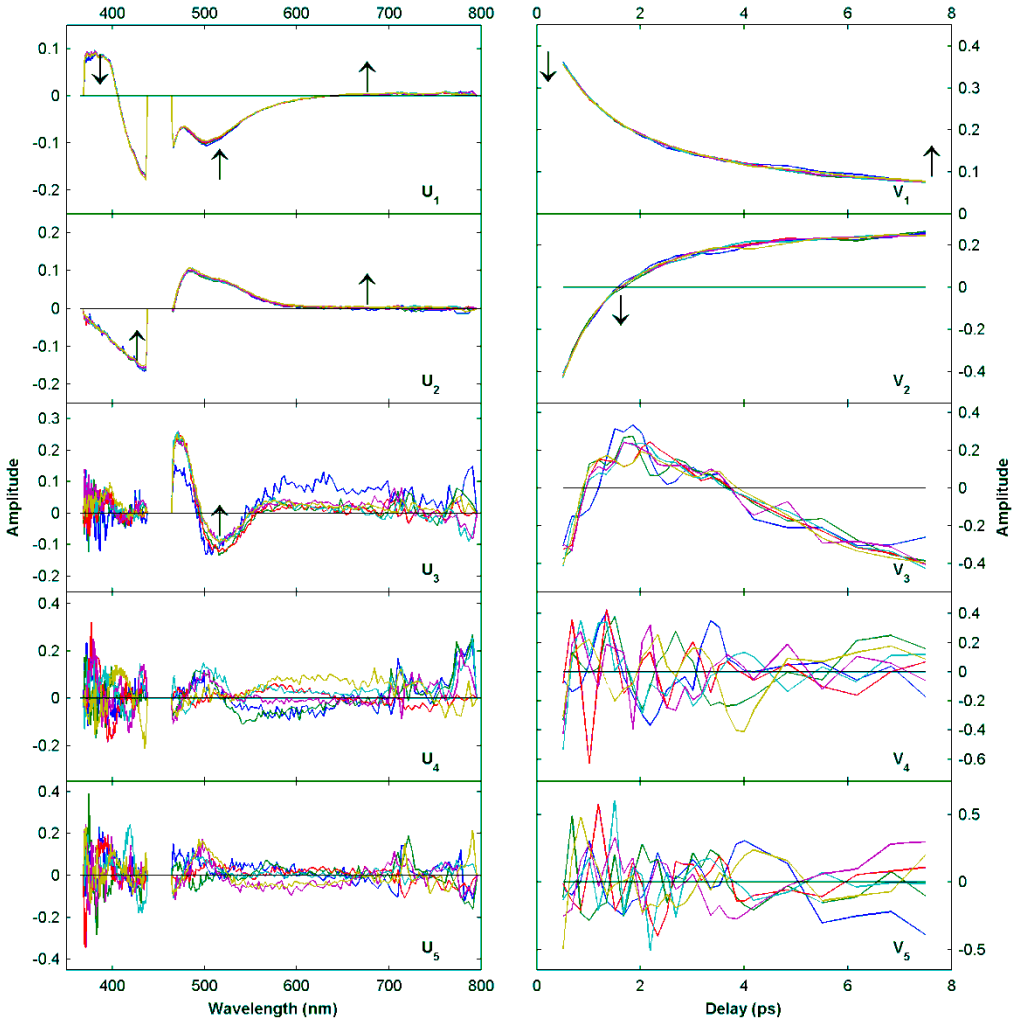

Fig. S27 SVD results of time-dependent transient absorption spectra of PYP excited with 450 nm, 300 fs pulses at six different excitation powers. The fit was applied only to delays greater than 0.4 ps to avoid early time artefact. Plotted are the left (U_i) and right (V_i) singular vectors for the first five singular values for each excitation power (arrows indicate increasing power). For clarity the singular values are plotted separately (Fig. S28). They are for the lowest power (9.1 GWcm^{-2}) 3.388, 0.856, 0.083, 0.070, 0.062 and the highest power (46.7 GWcm^{-2}) 8.767, 2.342, 0.212, 0.083, 0.066.

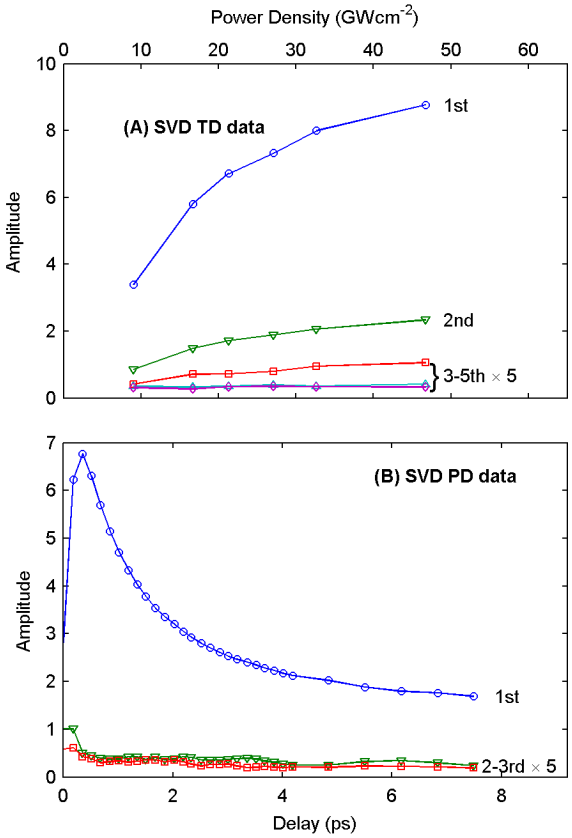

Fig. S28 First 5 singular values of SVD analysis of time-dependent transient absorption spectra of PYP excited at 450 nm and 300 fs pulses plotted against the six different excitation powers, see figure S27 for more detail. B) First three singular values of SVD analysis of power-dependent transient absorption spectra of PYP excited at 450 nm and 300 fs plotted against each measured delay time, see figure S29 for details.

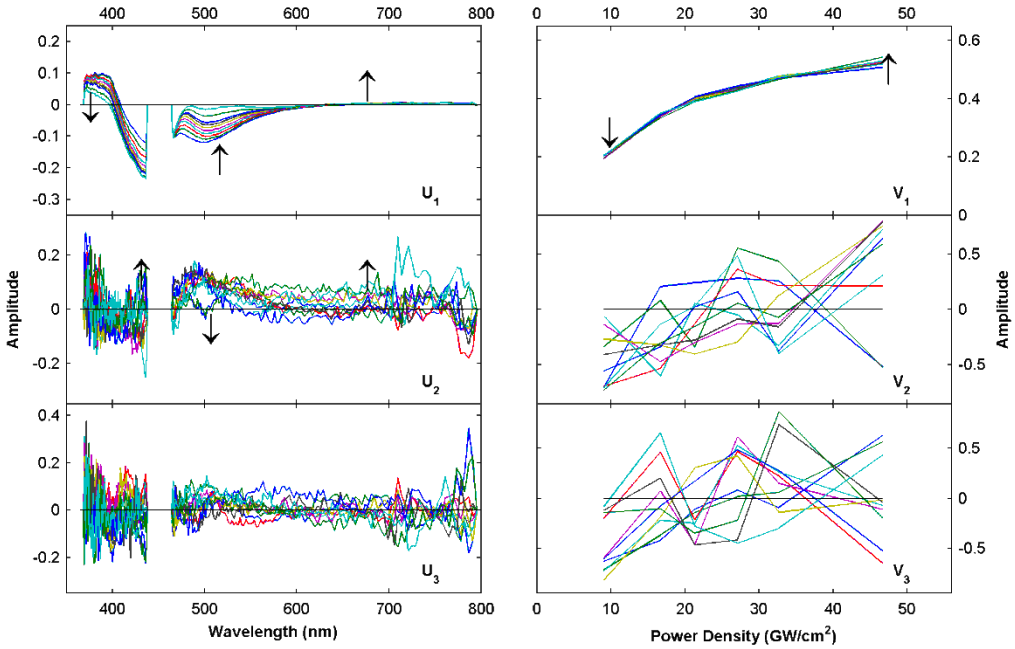

Fig. S29 Results of SVD of power-dependent transient absorption spectra of PYP excited with 450 nm, 300 fs and ten time delays between 0.4 and 7.5 ps. Plotted are the left (U_i) and right (V_i) singular vectors for the first three singular values (arrows indicate increasing time delay). For clarity the singular values are plotted separately (Fig. S28). The singular values are 6.306, 0.091, 0.077 (0.5 ps delay) and 1.689, 0.0472, 0.038 (7.5 ps delay).

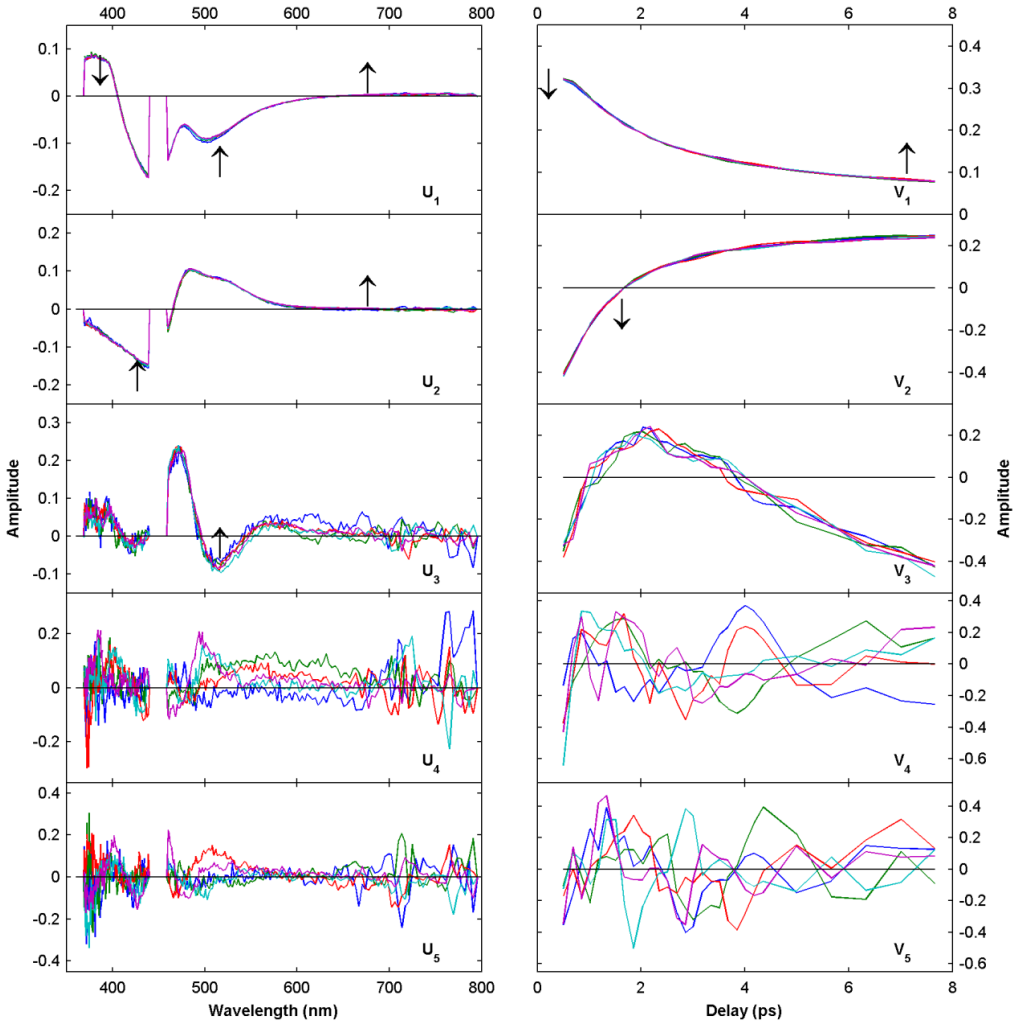

Fig. S30 SVD results of time-dependent transient absorption spectra of PYP excited with 450 nm, 600 fs pulses at five different excitation powers. The fit was applied only to delays greater than 0.4 ps to avoid early time artefact. Plotted are the left (U_i) and right (V_i) singular vectors for the first five singular values for each excitation power (arrows indicate increasing power). For clarity the singular values are plotted separately (Fig. S31). They are for the lowest power (4.3 GWcm^{-2}) 3.973, 1.021, 0.095, 0.047, 0.039 and the highest power (20.2 GWcm^{-2}) 9.197, 2.506, 0.203, 0.067, 0.057.

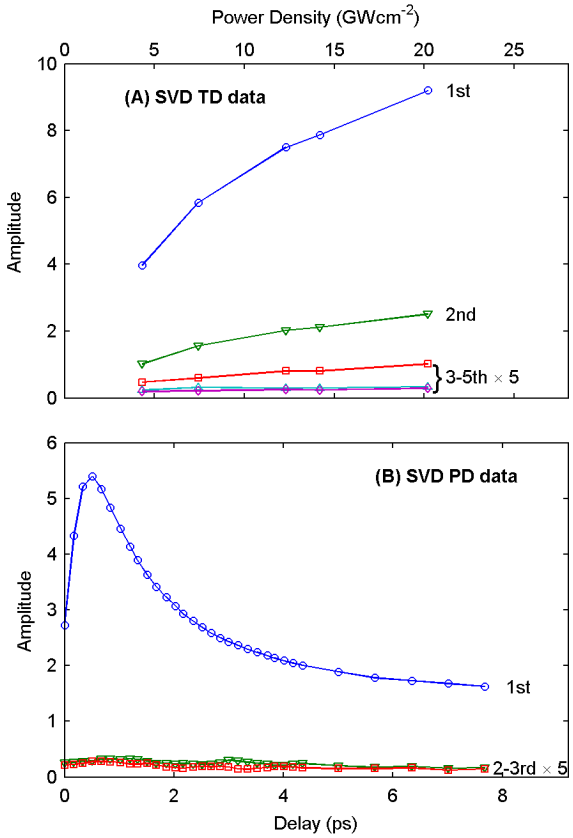

Fig. S31 First 5 singular values of SVD analysis of time-dependent transient absorption spectra of PYP excited at 450 nm and 600 fs pulses plotted against the five different excitation powers, see figure S30 for more detail. B) First three singular values of SVD analysis of power-dependent transient absorption spectra of PYP excited at 450 nm and 600 fs plotted against each measured delay time, see figure S32 for details.

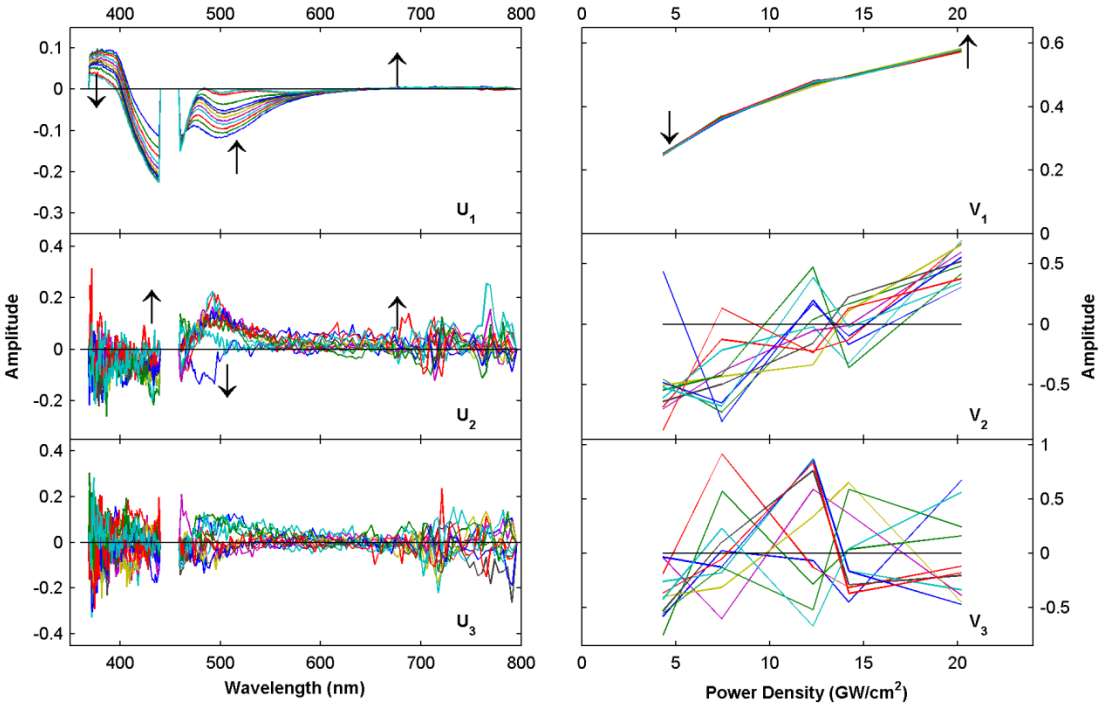

Fig. S32 Results of SVD of power-dependent transient absorption spectra of PYP excited with 450 nm, 600 fs and ten time delays between 0.4 and 7.5 ps. Plotted are the left (U_i) and right (V_i) singular vectors for the first three singular values (arrows indicate increasing time delay). For clarity the singular values are plotted separately (Fig. S31). The singular values are 5.392, 0.057, 0.055 (0.5 ps delay) and 1.626, 0.033, 0.029 (7.5 ps delay).

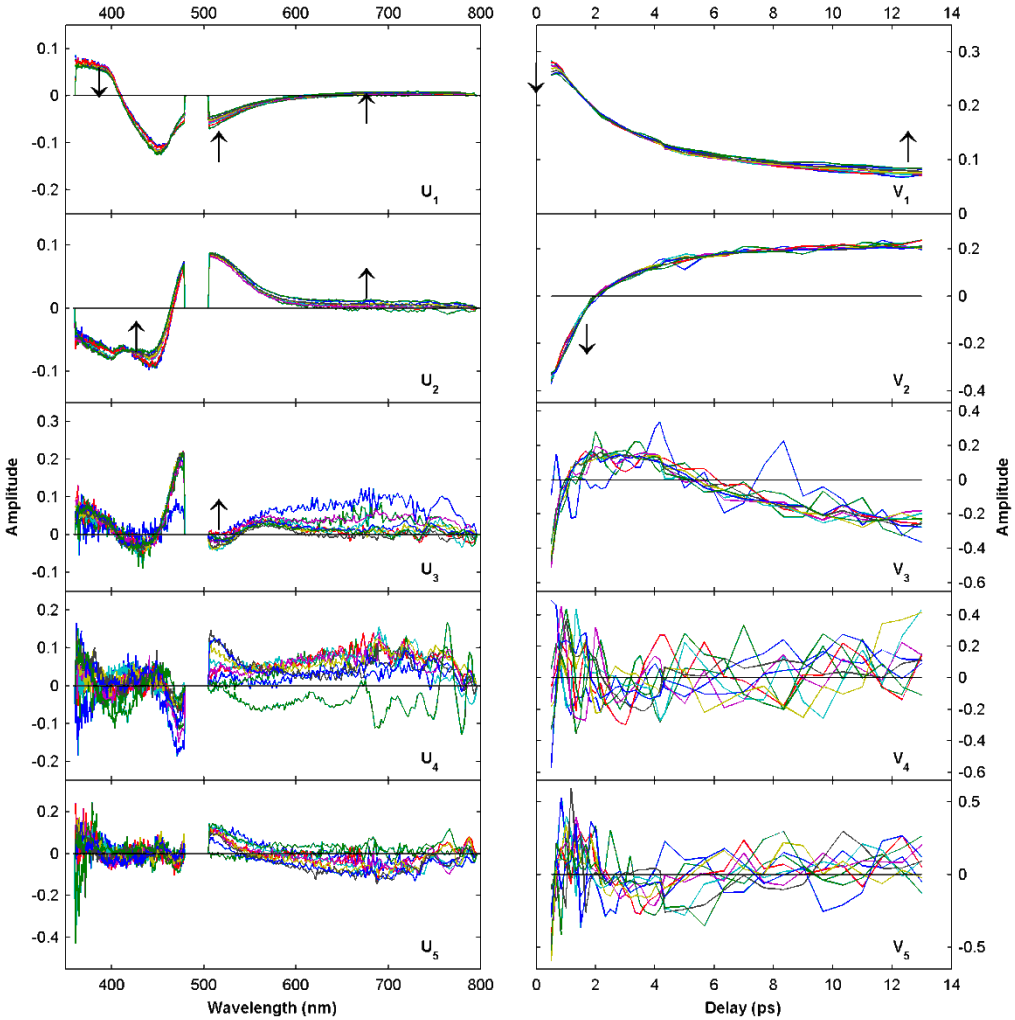

Fig. S33 SVD results of time-dependent transient absorption spectra of PYP excited with 490 nm, 300 fs pulses at nine different excitation powers. The fit was applied only to delays greater than 0.4 ps to avoid early time artefact. Plotted are the left (U_i) and right (V_i) singular vectors for the first five singular values for each excitation power (arrows indicate increasing power). For clarity the singular values are plotted separately (Fig. S34). They are for the lowest power (26.6 $GWcm^{-2}$) 0.936, 0.185, 0.026, 0.020, 0.013 and the highest power (294 $GWcm^{-2}$) 2.781, 0.611, 0.085, 0.025, 0.022.

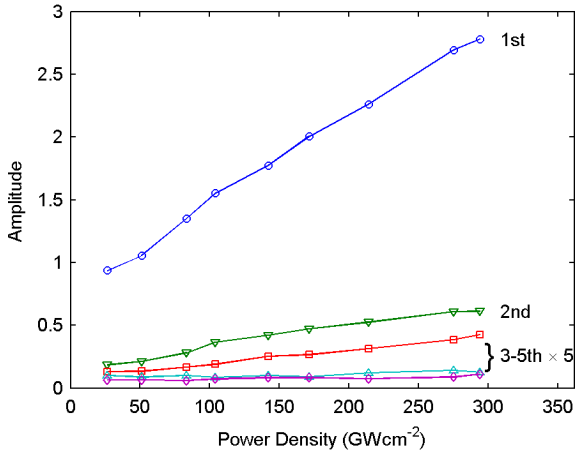

Fig. S34 First 5 singular values of SVD analysis of time-dependent transient absorption spectra of PYP excited at 490 nm and 300 fs pulses plotted against the nine different excitation powers, see figure S33 for more detail.

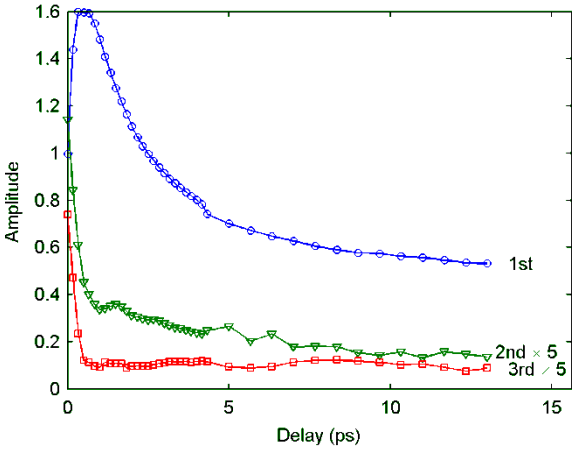

Fig. S35 First three singular values of SVD analysis of power-dependent transient absorption spectra of PYP excited at 490 nm and 300 fs plotted against each measured delay time, see figure S36 for details.

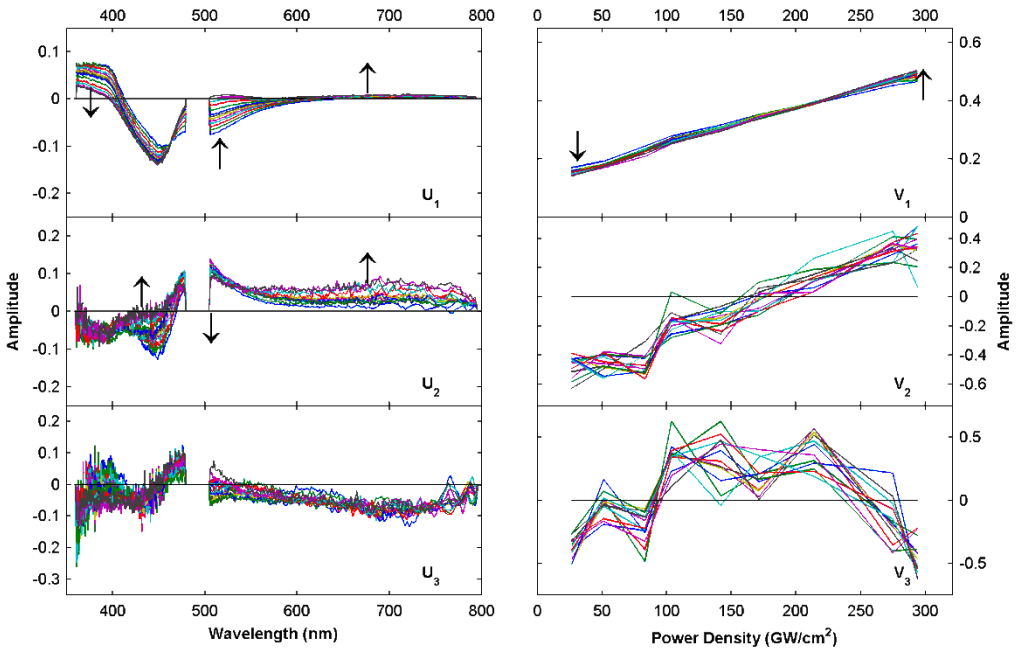

Fig. S36 Results of SVD of power-dependent transient absorption spectra of PYP excited with 490 nm, 300 fs and thirteen time delays between 0.4 and 13 ps. Plotted are the left (U_i) and right (V_i) singular vectors for the first three singular values (arrows indicate increasing time delay). For clarity the singular values are plotted separately (Fig. S35). The singular values are 1.595, 0.090, 0.024 (0.5 ps delay) and 0.532, 0.027, 0.017 (13 ps delay).